Anal. Chem. **2009,** *81,* 9055–9064

Reagentless Bidirectional Lateral Flow Bioactive Paper Sensors for Detection of Pesticides in Beverage and Food Samples

S. M. Zakir Hossain, Roger E. Luckham, Meghan J. McFadden, and John D. Brennan*

Department of Chemistry & Chemical Biology, McMaster University, 1280 Main Street West, Hamilton, ON L8S 4M1

A reagentless bioactive paper-based solid-phase biosensor was developed for detection of acetylcholinesterase (AChE) inhibitors, including organophosphate pesticides. The assay strip is composed of a paper support (1 × 10 cm), onto which AChE and a chromogenic substrate, indophenyl acetate (IPA), were entrapped using biocompatible sol−gel derived silica inks in two different zones (e.g., sensing and substrate zones). The assay protocol involves first introducing the sample to the sensing zone via lateral flow of a pesticide-containing solution. Following an incubation period, the opposite end of the paper support is placed into distilled deionized water (ddH_2O) to allow lateral flow in the opposite direction to move paper-bound IPA to the sensing area to initiate enzyme catalyzed hydrolysis of the substrate, causing a yellow-to-blue color change. The modified sensor is able to detect pesticides without the use of any external reagents with excellent detection limits (bendiocarb ∼1 nM; carbaryl ∼10 nM; paraoxon ∼1 nM; malathion ∼10 nM) and rapid response times (∼5 min). The sensor strip showed negligible matrix effects in detection of pesticides in spiked milk and apple juice samples. Bioactive paper-based assays on pesticide residues collected from food samples showed good agreement with a conventional mass spectrometric assay method. The bioactive paper assay should, therefore, be suitable for rapid screening of trace levels of organophosphate and carbamate pesticides in environmental and food samples.

There is widespread interest in the development of cost-effective, practical diagnostic tools that are amenable to rapid screening of specific target analytes in the health sector, food industry, and the environment.[1−9] Paper, being relatively cheap and abundant, sustainable, disposable, and easy to use, store, transport, and modify, has been the focus of significant attention as a platform for the development of paper-based analytical devices.[10−14] Paper also has the unique property of being able to move fluids by capillary action without the need for power and effect separation of components in mixtures. As a result, paper-based patterned microfludic as well as lateral flow colorimetric biosensing platforms have been developed, where multiple bioassays and controls are run simultaneously, in separate compartments, using hydrophobic channels on an absorbent paper surface to direct analyte solutions into well-defined sensing areas.[14−22] These portable colorimetric biosensing papers could be extremely useful in remote settings or developing countries where simple bioassays are essential in the first stages of detecting disease and for monitoring environmental- and food-based toxins in the field.[11,14] However, while these bioactive paper sensors show promise, most paper-based sensors reported to date have utilized biorecognition elements that are physically adsorbed onto the paper surface, which can be of limited use in terms of retaining long-term bioactivity of fragile biomolecules such as enzymes.

Recently, our group reported a novel bioactive paper-based sensing platform that utilizes immobilization of biorecognition

* To whom correspondence should be addressed. Tel: (905) 525-9140 (ext. 27033). Fax: (905) 527-9950. E-mail: brennanj@mcmaster.ca. Internet: http://www.chemistry.mcmaster.ca/faculty/brennan.

(1) Mabey, D.; Peeling, R. W.; Ustianowski, A.; Perkins, M. D. *Nat. Rev. Microbiol.* **2004**, *2*, 231–240.
(2) Whitesides, G. M. *Nature* **2006**, *442*, 368–373.
(3) Chin, C. D.; Linder, V.; Sia, S. K. *Lab Chip* **2007**, *7*, 41–57.
(4) Yager, P.; Edwards, T.; Fu, E.; Helton, K.; Nelson, K.; Tam, M. R.; Weigl, B. H. *Nature* **2006**, *442*, 412–418.
(5) Haeberle, S.; Zengerle, R. *Lab Chip* **2007**, *7*, 1094–1110.
(6) Gardeniers, J. G. E.; van den Berg, A. *Anal. Bioanal. Chem.* **2004**, *378*, 1700–1703.
(7) Willis, R. C. *Anal. Chem.* **2006**, *78*, 5261–5265.
(8) Daar, A. S.; Thorsteinsdóttir, H.; Martin, D. K.; Smith, A. C.; Nast, S.; Singer, P. A. *Nat. Genet.* **2002**, *32*, 229–232.
(9) Sia, S. K.; Linder, V.; Parviz, B. A.; Siegel, A.; Whitesides, G. M. *Angew. Chem., Int. Ed. Engl.* **2004**, *43*, 498–502.
(10) Zhao, W.; Ven den Berg, A. *Lab Chip* **2008**, *8*, 1988–1991.
(11) Martinez, A. W.; Phillips, Carrilho, E.; Thomas III, S. W.; Sindi, H.; Whitesides, G. M. *Anal. Chem.* **2008**, *80*, 3699–3707.
(12) Zhao, W.; Ali, M. M.; Aguirre, S. D.; Brook, M. A.; Li, Y. *Anal. Chem.* **2008**, *80*, 8431–8437.
(13) Aikio, S.; Grönqvist, S.; Hakola, L.; Hurme, E.; Jussila, S.; Kaukoniemi, O.-V.; Kopola, H.; Känsäkoski, M.; Leinonen, M.; Lippo, S.; Mahlberg, R.; Peltonen, S.; Qvintus-Leino, P.; Rajamäki, T.; Ritschkoff, A.-C.; Smolander, M.; Vartiainen, J.; Viikari, L.; Vilkman, M. *VTT-Work-51* **2006**, 1–84.
(14) Martinez, A. W.; Phillips, S. T.; Butte, M. J.; Whitesides, G. M. *Angew. Chem., Int. Ed.* **2007**, *46*, 1318–1320.
(15) Li, X.; Tian, J.; Nguyen, T.; Shen, W. *Anal. Chem.* **2008**, *80*, 9131–9134.
(16) Abe, K.; Suzuki, K.; Citterio, D. *Anal. Chem.* **2008**, *80*, 6928–6934.
(17) Bruzewicz, D. A.; Reches, M.; Whitesides, G. M. *Anal. Chem.* **2008**, *80*, 3387–3392.
(18) Su, S.; Ali, M. M.; Filipe, C. D. M.; Li, Y.; Pelton, R. *Biomacromolecules* **2008**, *9*, 935–941.
(19) Martinez, A. W.; Phillips, S. T.; Whitesides, G. M. *Proc. Natl. Acad. Sci. U.S.A.* **2008**, *105*, 19606–19611.
(20) Carrilho, E.; Phillips, S. T.; Vella, S. J.; Martinez, A. W.; Whitesides, G. M. *Anal. Chem.* **2009**, *81*, 5990–5998.
(21) Fenton, E. M.; Mascarenas, M. R.; Lopez, G. P.; Sibbett, S. S. *ACS Appl. Mater. Interfaces* **2009**, *1*, 124–129.
(22) Martinez, A. W.; Phillips, S. T.; Wiley, B. J.; Gupta, M.; Whitesides, G. M. *Lab Chip* **2008**, *8*, 2146–2150.

10.1021/ac901714h CCC: $40.75
Published on Web 09/29/2009

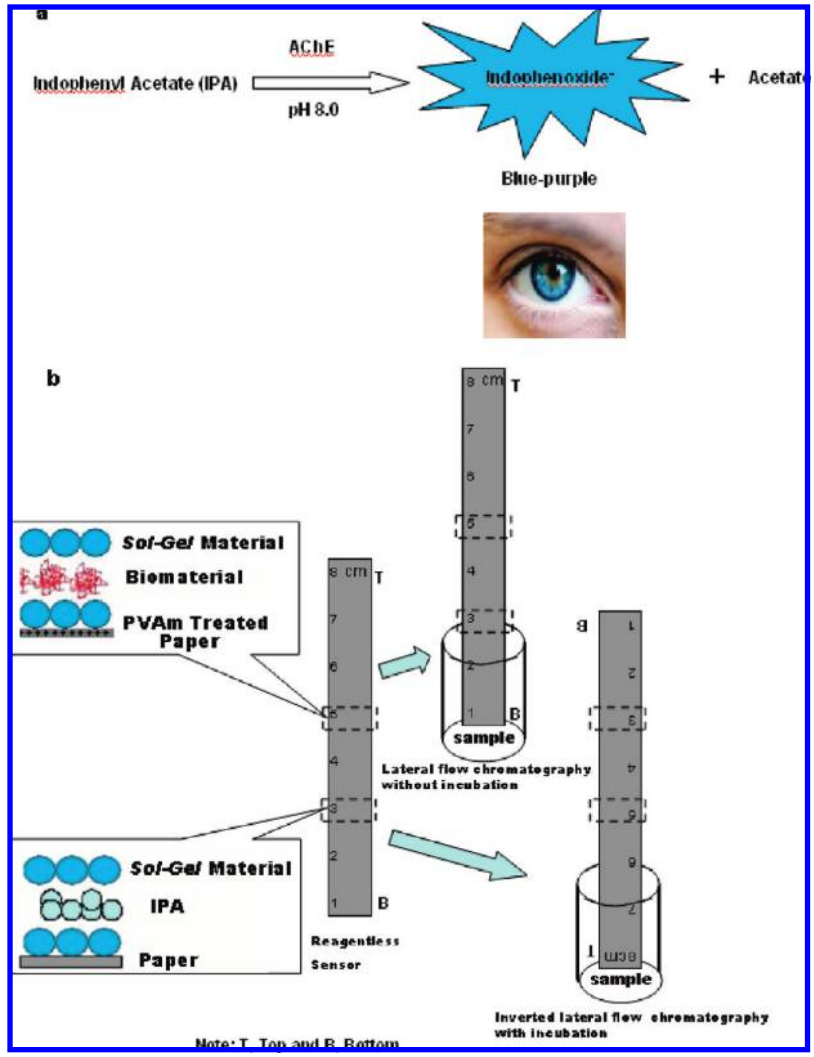

Figure 1. (a) Schematic diagram of the detection principle of the indophenyl acetate (IPA)-based colorimetric assay. Acetylcholinesterase (AChE) hydrolyzes the red-yellow colored substrate IPA under slightly basic conditions (pH 8.0) and forms indophenoxide anion, which is blue-purple in color. (b) Schematic illustration for the development of the reagentless bioactive paper-based lateral flow sensor in which AChE and IPA were entrapped in the two dashed box regions on a Whatman #1 paper strip (1 × 10 cm) following the sequences of PVAm/silica/AChE/silica and silica/IPA/silica, respectively, by the use of either inkjet printing or over spotting. The sensor can be used two different ways: (1) directly (normal lateral flow-based assay) without incubating the contaminated sample and (2) inverted lateral flow-based assay with incubation of the sample.

elements (e.g., enzymes) via piezoelectric inkjet printing of the enzyme within biocompatible sol−gel derived silica layers onto paper supports.[23] In this study, the enzyme acetylcholinesterase (AChE) was deposited and used for the detection of AChE substrates and inhibitors based on Ellman's colorimetric assay. With this system, the sol−gel matrix efficiently entrapped the biomolecule while enabling small molecules to diffuse into and out of the matrix, thus allowing for use in either a lateral flow or dipstick format. The assay provided good detection limits (paraoxon ~100 nM; aflatoxin B1 ~1 nM) and rapid response times (<5 min). However, this paper-based assay system required the addition of an external reagent, acetylthiocholine (ATCh), for each assay, as the reagent could not be printed onto the paper owing to relatively rapid (<3 h) autohydrolysis upon storage. Furthermore, the bioactive paper assay was not well-suited for detection of inhibitors that required extended incubation times. These drawbacks limited the potential use of this solid-phase sensor in the field or in emergency situations.

In the present study, we report on a fully integrated reagentless paper-based lateral flow device which employs biocompatible sol−gel-derived silica as an entrapment agent to deposit not only the enzyme but also all other required reagents onto a paper support via piezoelectric inkjet printing. Figure 1a illustrates the detection principle, which utilizes an indophenyl acetate (IPA)-based colorimetric assay.[24] Acetylcholinesterase (AChE) hydrolyzes the red-yellow colored substrate, IPA, to the blue-purple indophenoxide anion (IDO^-) which is then trapped over a finite region by the cationic polymer, polyvinyl amine (PVAm). The absence or decrease in blue-purple color, over this region, is indicative of the presence of AChE inhibitors. The paper-based lateral flow sensor requires only immersion into water for

(23) Hossain, S. M. Z.; Luckham, R. E.; Smith, A. M.; Lebert, J. M.; Davies, L. M.; Pelton, R. H.; Filipe, C. D. M.; Brennan, J. D. *Anal. Chem.* **2009**, *81*, 5474–5483.

(24) Kramer, D. N.; Gamson, R. M. *Anal. Chem.* **1958**, *30*, 251–254.

proper functioning, as all reagents are deposited onto the paper surface with good long-term stability. As part of the optimization process, we investigated PVAm levels, pH effects on IPA stability, the effect of paper support, and IPA and enzyme concentration on signal output, as well as the effect of various sample matrixes on the sensitivity of the assay platform. The performance of the sensor under optimized conditions was assessed in two ways: (1) directly (normal lateral flow-based assay) without incubation of the contaminated sample and (2) using an inverted lateral flow-based assay to allow incubation of the sample. The latter format exploits a unique feature of paper as a lateral flow device, which is the ability to move liquids in both directions along the paper support. This allows for a "bidirectional" lateral flow assay to provide an opportunity to incubate inhibitors in samples prior to introducing substrate to generate a signal. In this case, inhibitors are first flowed directly into the AChE reaction area without exposure to IPA by immersing the top of the strip into the sample, and then, the strip is inverted and the bottom of the strip is immersed into ddH_2O to move IPA to the sensing area of the strip and generate a signal, as shown in Figure 1b. We show that the sensor can be used for rapid, reagentless sensing of pesticides present in beverages or on food samples and demonstrate that the data obtained from pesticide residues on food samples correlate well with data obtained using a conventional electrospray-tandem mass spectrometry (ESI-MS/MS) assay. Finally, we demonstrate that the reagentless sensor has a sufficiently long shelf life to permit shipment and use in remote locations.

EXPERIMENTAL SECTION

Reagents. All chemicals from commercial sources were of analytical grade and used without further purification. Sodium silicate solution (~14% NaOH, ~27% SiO_2), Dowex 50WX8−100 ion-exchange resin, acetylcholinesterase (AChE, from *Electrophorus electricus*, EC 3.1.1.7), Triton X-100, and pesticides including both organophosphates (OP) (e.g., paraoxon and malathion) and carbamates (CM) (e.g., carbaryl and bendiocarb), as well as galanthamine hydrobromide (a well-known inhibitor of AChE) from *Lycoris* sp., were obtained from Sigma-Aldrich (Oakville, ON, Canada). Indophenyl acetate (IPA) was purchased from Pfaltz & Bauer, Inc. (Waterbury, CT). Polyvinylamine (PVAm; 1.5 MDa) was obtained from BASF (Mississauga, Canada), as a gift. Anhydrous glycerol was purchased from Fluka BioChemika Ultra (Dorset, U.K.). Distilled deionized water was obtained from a Milli-Q Synthesis A10 water purification system.

Solution Preparation. Stock solutions of IPA, bendiocarb, carbaryl, paraoxon, malathion, and galathamine were made up daily and were not used for more than 3 h after preparation to minimize the potential for degradation. A mixture of Tris buffer (10 mM, pH 6.8) and 5% methanol (Sigma) was used for dissolving bendiocarb, carbaryl, malathion, paraoxon, and galanthamine while a mixture of Tris buffer (10 mM) at pH 8.0 with 5% methanol (Sigma) was used for making IPA stock solutions. These solvents not only aided in dissolution of the AChE inhibitors but also enhanced the affinity of pesticides for binding to AChE.[25−27] Furthermore, this level of organic solvent has been shown not to affect the stability of AChE. Distilled deionized water (ddH_2O) was used to dissolve PVAm. All other solutions were prepared using Tris buffer (10 mM, pH 8.0), if not otherwise stated. *CAUTION: Both carbamate (e.g., bendiocarb, carbaryl) and organophosphate (e.g., paraoxon, malathion) pesticides, as well as galanthamine, are extremely toxic. These materials should be handled with gloves and masks and used in a fume hood.*

Sol−Gel Material Preparation. The biocompatible sol−gel precursor sodium silicate (SS) was used to prepare sols for both enzyme and IPA entrapment onto paper. SS sols were prepared by mixing 10 mL of ddH_2O with 2.6 g of sodium silicate solution (pH ~13) followed by addition of 5 g of Dowex cation exchange resin to replace Na^+ with H^+. The mixture was stirred for 30 s to reach a final pH of ~4 and then vacuum filtered through a Büchner funnel. The filtrate was then further filtered through a 0.45 μm membrane syringe filter. These sols were used to prepare silica-containing inks, as described below.

Fabrication of Reagentless Bioactive Paper-Based Lateral Flow Sensor. A section of Whatman #1 paper was cut into small pieces (1 × 10 cm) on which AChE and IPA were entrapped in two different regions (e.g., sensing and substrate regions). The sensing region was prepared by depositing PVAm (0.5 wt %)/silica/AChE/silica layers in the order described, while the substrate region was prepared by depositing silica/IPA/silica layers using either inkjet printing (using a piezoelectric inkjet printer (DMP-2800), Fujifilm Dimatix, Inc. (Tokyo, Japan) or deposition via pipet (for proof-of-concept studies and assay optimization), as shown in Figure 1b. In the case of inkjet printing, all inks were modified with respect to viscosity and surface tension using 30% glycerol (v/v) and 0.1 wt % Triton X-100, respectively, and printing was done, as reported previously.[23] After printing, the sensor was allowed to dry for at least 1 h in air at room temperature. For control experiments, a buffer that did not contain AChE was entrapped between the silica layers in the sensing region or a buffer that did not contain IPA was entrapped between the silica layers in the substrate region. Other controls involved entrapment of AChE directly onto the PVAm underlayer without a silica coating and entrapment of AChE onto PVAm/silica without printing a silica overlayer.

Optimization of Reagentless Paper-Based Lateral Flow Assay Platform. The effects of assay pH, PVAm, IPA, and enzyme concentration were examined to optimize the lateral flow assay. The effect of pH on IPA stability was initially investigated in solution. For this, IPA (3 mM) was dissolved with Tris buffer having different pH values (4−9.5). IPA solution (80 μL) and AChE (20 μL, final concentration of 500 U/mL) were mixed into a 96-well plate and incubated for 5 min to allow color development. The absorbance at 640 nm was then measured using a TECAN Safire microwell plate reader.

Prior to monitoring AChE activity on paper, the activity of AChE as a function of enzyme and IPA concentration was optimized in silica monoliths present in 96-well plates. Different concentrations of AChE (0−1500 U/mL) were entrapped in SS + 30% glycerol in a 96-well plate (total volume of 80 μL). Twenty microliters of IPA (0−5 mM) was then added into each well and

(25) Fennouh, S.; Casimiri, V.; Burstein, C. *Biosen. Bioelectron.* **1997**, *12*, 97–104.
(26) Zhang, C.; Malhotra, S. V. *Talanta* **2005**, *67*, 560–563.
(27) Arduini, F.; Errico, I.; Amine, A.; Micheli, L.; Palleschi, G.; Moscone, D. *Anal. Chem.* **2007**, *79*, 3409–3415.

incubated for 5 min to allow color development. The absorbance at 640 nm was then measured using a TECAN Safire plate reader.

AChE activity was optimized on the bioactive paper strip by measuring the color intensity produced by the enzymatic hydrolysis of IPA. PVA (0.5 wt %)/silica/AChE/silica layers were printed at a width of 0.5 cm across the paper and 4 cm from the bottom of the paper, as described previously[23] (AChE concentration of 500 U/mL), while silica/IPA/silica layers were printed in a 1 cm wide area across the paper strip and 2 cm from the bottom of the paper (IPA concentration of 3 mM in 30% glycerol with 0.1 wt % Triton X-100). Note that relatively high concentrations of AChE and IPA were required for these assays, as IPA is a relatively poor substrate for the enzyme. PVAm concentration was optimized by depositing 0−1 wt % solutions of PVAm onto the sensing layer prior to deposition of silica/AChE/silica layers and by performing lateral flow assays of the IPA and measuring color intensity, as described below.

The performance of the sensor under optimized conditions was assessed in two ways: (1) directly (normal lateral flow-based assay) without incubating the contaminated sample and (2) inverted lateral flow-based assay (also referred to as bidirectional lateral flow) to allow incubation of the sample over the sensing area. In the former case, the bottom of the paper strip was placed in solution to allow the sample and IPA to reach the AChE at the same time. For the latter case, the top of the paper was first placed into the sample solution and removed as soon as the sample reached the sensing region, followed by a 5 min incubation time in air at room temperature. The sensor was then inverted and the bottom of the strip was immersed into ddH_2O to bring IPA up to the sensing area via lateral flow. AChE hydrolyzes the chromogenic substrate IPA at pH 8.0 to produce a highly blue colored product. A decrease in color formation indicates the presence of an inhibitory substance.

The color intensity of the sensing areas was quantified by obtaining a digital image (Canon A630, 8.0 MegaPixel camera operated in automatic mode with no flash and using the macro-imaging setting) and using ImageJ software to analyze the jpeg images. The wet paper strip was allowed to dry in air for 3 min before taking the digital images. Stable colorimetric signals were observed after this period. ImageJ software uses a 256 bit color scale, and for image processing, the images were inverted so that white corresponded to a color intensity of zero and black corresponded to 256. Using this scale, increases in the amount of blue color cause an increase in color intensity of our reagentless sensor strips. To account for variations in color intensity owing to differences in environmental illumination, a background subtraction (color intensity of the paper surface closest to the sensing area) was done for each data point.

Measurement of Pesticides Using Reagentless Paper-Based Lateral Flow Assays. The inhibitory effects of carbamate (e.g., bendiocarb, carbaryl) and organophosphate (e.g., paraoxon, malathion) pesticides, as well as the inhibitor galanthamine, were evaluated on the reagentless paper-based sensor by measuring the decrease in the color intensity produced in IPA-based colorimetric assays. The sensing area of the bioactive paper strip was first incubated with various concentrations of carbamate, organophosphate, or galanthamine solution for 5 min following the inverted lateral flow procedure, as described above. The sensor was then inverted and immersed into ddH_2O (as mentioned above) for testing the performance of the sensor strips. The color intensity was determined by analyzing a digital image with the ImageJ software, as described above. *CAUTION: These assays should be performed in a fume hood using appropriate protective apparel.*

Matrix Effect in the Analysis of Paraoxon in Beverages. The matrix effects in the analysis of paraoxon in milk (2%, pH 7.2) and apple juice (pH 3.6) samples were investigated. Several standard paraoxon solutions were mixed into both milk (10 mL) and apple juice (10 mL) samples, resulting in final paraoxon concentrations of 0−10 μM. Prior to analysis, the pH of the apple juice was adjusted to between 7 and 8 by adding a few drops of 1 N NaOH. Milk samples were tested with no additional processing. In both cases, the top of each reagentless sensor was immersed into each of the paraoxon containing samples to move the sample to the sensing area by lateral flow (Figure 1b). The sensor was incubated for 5 min, and the inhibition of AChE was tested by introducing the bottom of the sensor strip into ddH_2O to move IPA to the sensing region. Color intensity was determined, as outlined above, and the data were used to produce a standard curve relating color intensity to paraoxon concentration.

Analysis of Paraoxon in Food Samples. Different concentrations of paraoxon solution (0−10 mM, 1 mL of each concentration) were sprayed onto the skin of apples (cut into two halves) or the surface of head lettuce (cut into four quarters), respectively. The samples of paraoxon residue were collected, after 48 h using a cotton swab, into 2 mL of ddH_2O and tested using the inverted lateral flow procedure outlined above with a 5 min incubation time. In order to verify our results, a fraction of sample (500 μL for each concentration) was filtered through a 0.22 μm filter, and the filtrate was analyzed by direct injection into an ESI-MS/MS instrument (LCQ FLEET, Thermo Scientific) using selected reaction monitoring (SRM) mode. Prior to analyzing the sample via mass spectrometry, a standard curve of paraoxon was obtained using different standard solutions (0.1−25 μM). The ESI-MS/MS operating conditions were as follows: sample loop, 10 μL; flow rate, 15 μL/min; spray voltage, 5.1 V; capillary temperature, 150 °C; capillary voltage, 46 V; parent (m/z) 276 and daughter (m/z) 248. The mobile phase was a mixture of isopropyl alcohol (Sigma) and HPLC grade H_2O (1:1) (Sigma) containing 1% acetic acid (v/v). The standard curve was constructed by monitoring the SRM signal over time after injection of the various paraoxon standards and plotting the area under the curve against paraoxon concentration.

Determination of Paraoxon Residue Levels with Time. A paraoxon solution (1 mM) was sprayed onto the skin of apples; the apples were cut in half and washed, as described above, to collect the paraoxon residue 1, 2, 3, 4, 5, 6, and 7 days after application using the procedure outlined above. The levels of paraoxon residue were then determined using the reagentless paper sensor in a bidirectional lateral flow assay, as described above.

Storage Stability of the AChE- and IPA-Immobilized Strip. The long-term stability of AChE and IPA on the paper strip (stored at 4 °C) was evaluated every week up to 4 weeks by immersing the test strip into ddH_2O to allow IPA to move into the sensing region and react with AChE (normal lateral flow-based assay as described above), with the signal quantified as described above.

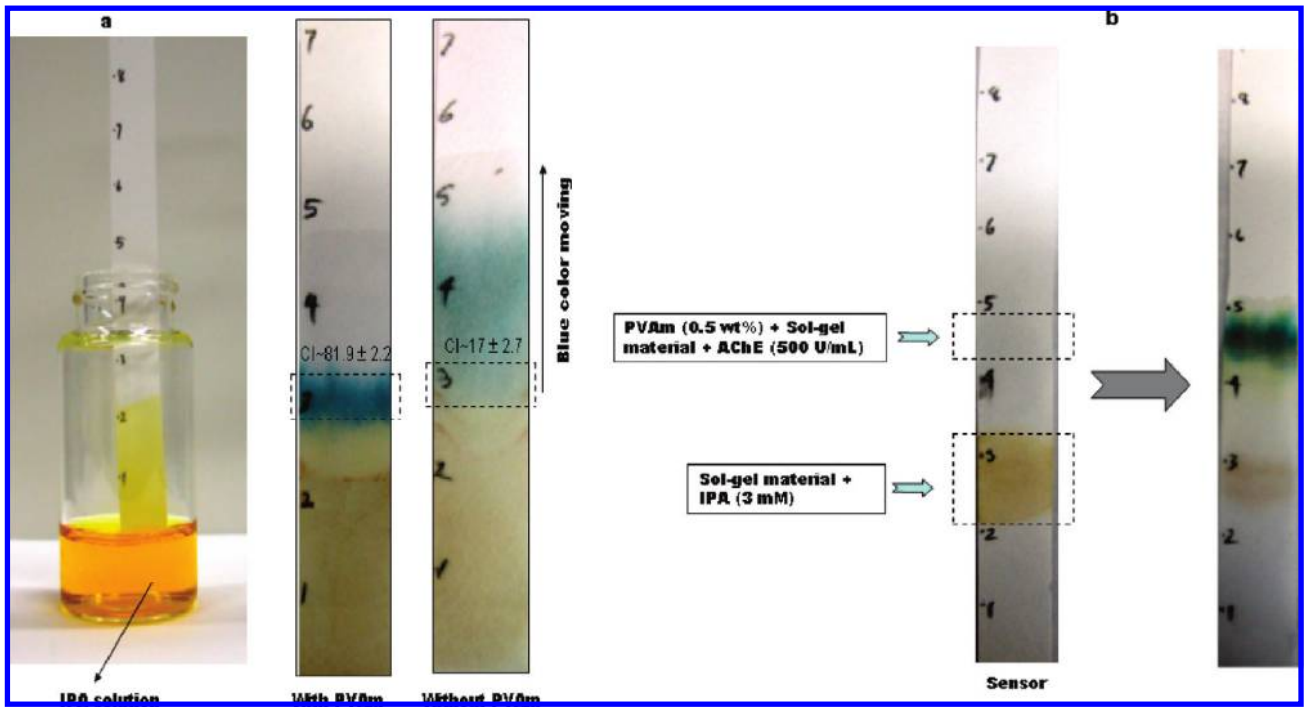

Figure 2. (a) Effects of cationic PVAm on entrapment of indophenoxide anion in a lateral flow-based paper sensor system. Color intensity (CI) due to elution of IPA (3 mM, final concentration) in the lateral flow-based platform. The areas within the dashed boxes were printed/over spotted without (control) and with PVAm (0.5 wt. %) followed by printing/overspotting of AChE (500 U/mL). PVAm concentrates the reaction product, the blue indophenoxide anion, while in the control experiment; the blue indophenoxide anion is dispersed over a large area. (b) Proof of concept for the development of the reagentless bioactive paper-based lateral flow platform, in which the sensor was dipped into ddH_2O to move the IPA reagent into the sensing region for the generation of the blue color.

RESULTS AND DISCUSSION

Optimization of the Reagentless Lateral-Flow Assay Format. Prior to developing an efficient, reagentless lateral flow paper-based sensor with high sensitivity and rapid response, all necessary parameters such as PVAm levels, pH of the buffer, and concentrations of substrate and enzyme were optimized. In our previous work,[23] we demonstrated that paper supports treated with 0.5 wt % PVAm were able to capture and concentrate the anionic product 5-thio-2-nitrobenzoate (TNB^-), which was produced through reduction of 5,5′-dithiobis-(2-nitrobenzoic acid) (DTNB) by thiocholine, the product of the AChE catalyzed hydrolysis of acetylthiocholine.[28] This level of PVAm also preserved the color after storage of more than 1 month.

To assess whether this level of PVAm was also able to capture and concentrate the IDO^- produced from AChE catalyzed hydrolysis of IPA, paper supports were printed with 0.5 wt % PVAm followed by overprinting of the silica and AChE layers and the sensors were immersed into an IPA solution. Figure 2a shows the color intensity (CI) due to IDO^- that is trapped within finite PVAm regions on the lateral flow device. The areas within the dashed boxes were either treated or not (control) with 0.5 wt % PVAm. The data indicated that the 0.5 wt % PVAm level was able to trap and concentrate the IDO^- efficiently without diminishing the color intensity, while the unmodified paper (control) failed to trap the blue color. The relative increase in color intensity with 0.5 wt % PVAm was ~5-fold, and thus, this level of PVAm was used in all further paper-based assays. The PVAm was also able to retain color produced by the IDO product over a period of at least 4 days, showing that the used sensors could be stored for a short period prior to imaging.

Figure 2b shows the signals obtained from a reagentless bioactive paper sensor, in which AChE and IPA were deposited in the two different regions (e.g., lower substrate region and upper sensing region) using either inkjet printing or manual addition. The bottom of the sensor was placed into ddH_2O which initiated movement of IPA by capillary action from the substrate region into the sensing region to generate the characteristic blue color of the IDO^- product resulting from enzymatic hydrolysis of IPA. The color change occurred in a matter of a few seconds, showing that the AChE catalyzed hydrolysis of IPA was not a rate limiting factor in the assay. This proof of concept study indicates that this mechanism is ideal for a reagentless bioactive lateral-flow paper-based sensing platform.

The hydrolysis of IPA is known to be pH sensitive, and therefore, optimization of pH is a key parameter for optimization of the sensor performance. Preliminary studies on the effects of pH over the range from 4 to 9.5 (in 10 mM Tris buffer) on IPA stability in solution showed that IPA is stable between pH 4 and 8.5 (supplementary Figure 1a in the Supporting Information). At pH levels above 8.5, IPA rapidly degrades owing to autohydrolysis.[24] Supplementary Figure 1b in the Supporting Information shows the changes in the IPA spectrum upon AChE catalyzed hydrolysis of IPA and demonstrates that absorbance increases of up to 5-fold are possible when measuring absorbance at 640 nm.

(28) Ellman, G. L.; Courtney, K. D.; Andres, V.; Featherstone, R. M. *Biochem. Pharmacol.* **1961**, *7*, 88–95.

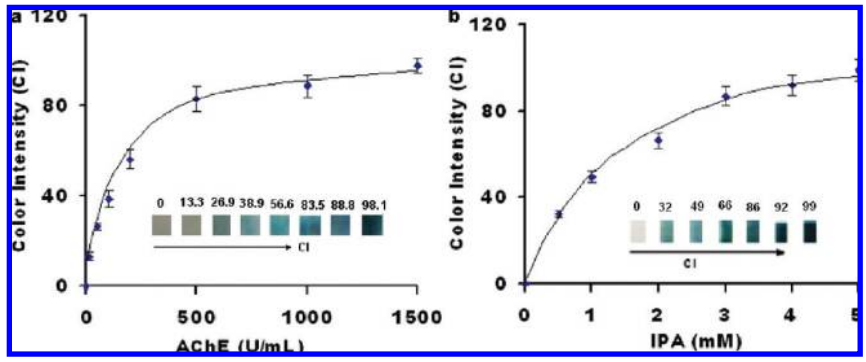

Figure 3. Optimization of [AChE] and [IPA] for the development of the paper-based lateral flow sensor. (a) Color intensity at different [AChE] in the presence of IPA (3 mM) on paper. (b) Effects of [IPA] in the presence of AChE (500 U/mL) doped SS sol−gel matrix on paper. All points are means ± s.d. of four measurements for each concentration, and all paper assays used 0.5 wt % PVAm as a capture agent. Color intensity values are shown above each image.

Supplementary Figure 1c in the Supporting Information shows the final absorbance of the AChE catalyzed hydrolysis of IPA as a function of pH. The data demonstrate that pH values below pH 6 were not compatible with maintenance of AChE activity, while maximum signal was obtained at pH 8 or higher. Thus, pH 8 was used for all further paper-based assays.

Prior to performing inhibition studies on paper, the activity of AChE as a function of both the concentration of enzyme (AChE; 0−1500 U/mL) and substrate (IPA; 0−5 mM) was also optimized in both 96-well format and on paper. Microwell plate assays performed in silica monoliths showed signal saturation at [AChE] = 500 U/mL and [IPA] = 3 mM (supplementary Figure 2 in the Supporting Information). The [AChE] and [IPA] were optimized further using our reagentless lateral flow paper-based sensor. For this, an ideal reagentless lateral flow paper-based sensor was constructed following the procedure as described above. The effects of [AChE] on signal levels at constant [IPA] (3 mM) is shown in Figure 3a (a separate paper sensor is used for each AChE concentration). Results were similar to those obtained from solution-based assays with signal saturation occurring at [AChE] ~ 500 U/mL. From these findings, 500 U/mL AChE was chosen as the best compromise between low enzyme loading, a sufficiently high signal (>7-fold increase over background), and good long-term stability. The high activity of entrapped AChE is in good agreement with previous reports showing that the enzyme is active and stable in sol−gel derived silica materials.[23,29] Figure 3b shows the effects of [IPA] on signal levels at constant [AChE] (500 U/mL; a separate paper sensor is used for each IPA concentration). Here, it is seen that as the concentration of IPA increases so too does the color intensity with saturation at [IPA] ~3 mM, which is similar to that obtained from the plate-based assay. Thus, 3 mM IPA was chosen for all other experiments, as this provides a good compromise between low reagent concentrations without significant loss of signal. Using the paper-based assay, the K_M for IPA was found to be ~1.4 mM which was similar to results obtained with the plate-based assay. This value was 2-fold higher than the literature value obtained in solution (~0.70 mM),[30] likely owing to diffusion limitations of the substrate though the silica matrix.[31]

Lastly, to ascertain whether or not the supporting silica material, paper substrate, or PVAm layers degraded IPA, similar experiments were conducted as described above with no AChE present. The responses remained at the baseline level upon addition of varying levels of IPA and were similar to signals obtained from control experiments performed in the absence of substrate (data not shown). Thus, our results confirm that the change in the color intensity is due to the enzyme catalyzed hydrolysis of IPA to IDO^- (blue colored product). Furthermore, this result shows that both the AChE and IPA remain active when deposited between silica layers on a paper substrate.

Performance of Reagentless Lateral-Flow Assay Platform for Toxin Sensing. Using optimum conditions, inhibition studies were performed using the bioactive paper sensors. It is well-known that pesticides such as carbamates (e.g., bendiocarb, carbaryl) and organophosphates (e.g., paraoxon, malathion) are potent inhibitors of AChE[25,26,32−34] and, even though banned in most developed countries, are still being used in developing countries. To assess whether our lateral flow paper-based biosensor was able to detect sublethal levels of these compounds, assays were conducted in two ways: (a) by dipping the test strip directly into solutions containing various levels of pesticides without incubating at room temperature and (b) by utilizing a bidirectional "inverted" flow system in which inhibitors are introduced to the sensing region from one end of the paper strip, and then the substrate is carried to the sensing region from the opposite end. Using this technique, test strips were incubated with inhibitors for 5 min after which time ddH_2O was used to move IPA to the sensing region. We found that the detection limit of pesticides was considerably better for preincubated test strips utilized in the bidirectional lateral flow format, with LOD levels being on the order of 10-fold better than was obtained for direct assays (data not shown). The improvement in sensitivity is most likely due

(29) Pandey, P. C.; Upadhyay, S.; Pathak, H. C.; Panday, C. M. D.; Tiwari, I. *Sens. Actuators, B* **2000**, *62*, 109–116.
(30) O'Brien, R. D. *J. Biochem.* **1969**, *118*, 713–719.
(31) Besanger, T. R.; Chen, Y.; Deisingh, A. K.; Hodgson, R.; Jin, W.; Stanislas, M.; Brook, M. A.; Brennan, J. D. *Anal. Chem.* **2003**, *75*, 2382–2391.
(32) Marrs, T. C. *Pharmacol. Ther.* **1993**, *58*, 51–66.
(33) Rosenfeld, C. A.; Sultatos, L. G. *Toxicol. Sci.* **2006**, *90*, 460–469.
(34) Beam, J. E.; Hankinson, D. J. *J. Dairy Sci.* **1964**, *47*, 1297–1305.

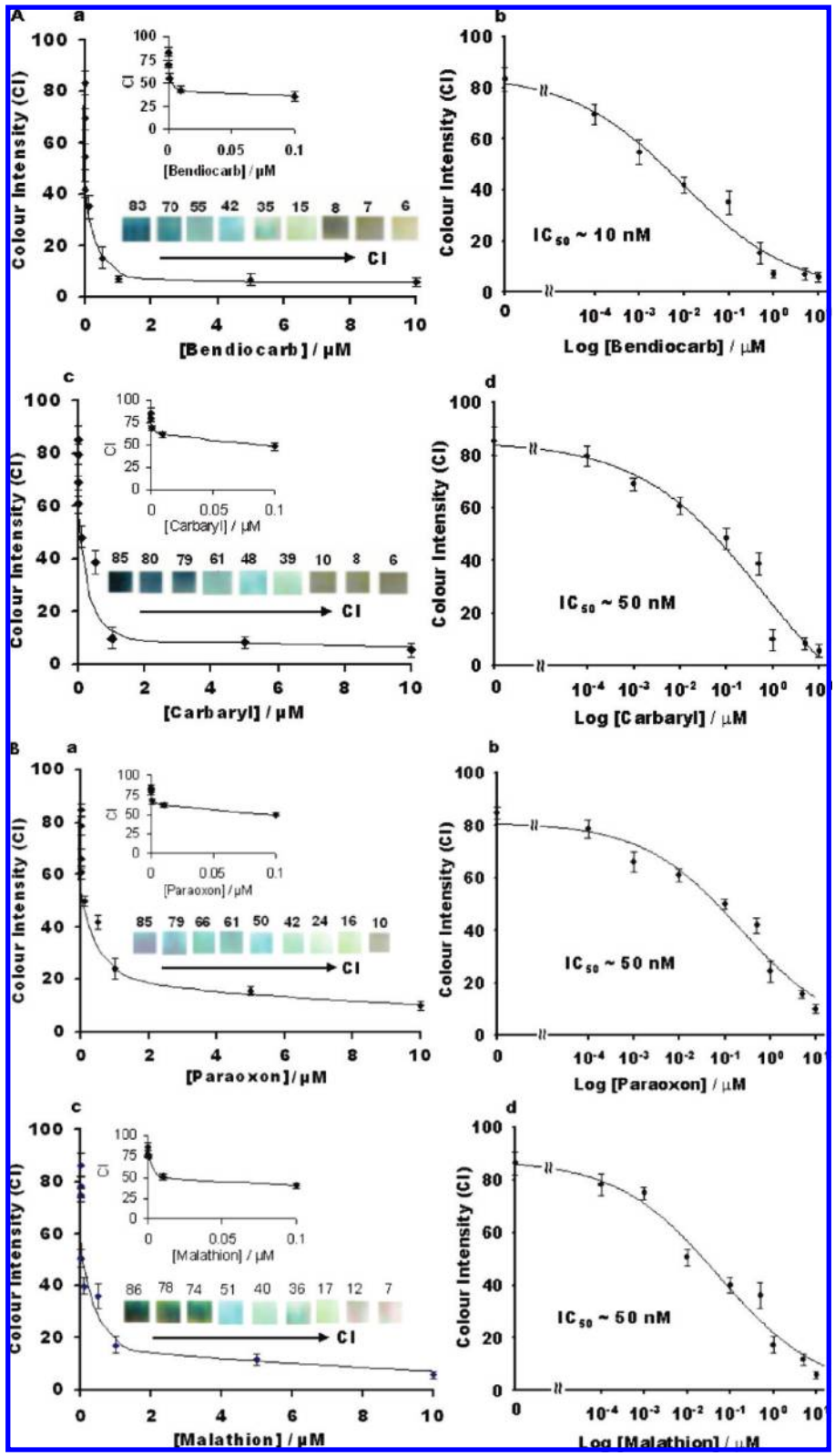

Figure 4. Dose-dependent inhibition of acetylcholinesterase (AChE) by various concentrations of carbamate (A) and organophosphate (B) pesticides. A-a and A-c show the dose-dependent inhibition responses of bendiocarb and carbaryl, respectively. A-b and A-d show the semilog plots of data in panels A-a and A-c, respectively. B-a and B-c show the dose-dependent inhibition responses of paraoxon and malathion, respectively. B-b and B-d show the semilog plots of data in panels B-a and B-c, respectively. Insets (left panels) are the color intensity (CI) at each pesticide concentration and dose-dependent inhibition responses with the lower levels of toxins. All points are means ± s.d. of four measurements for each concentration.

to the fact that an increased incubation time allows the inhibitor to penetrate through the thin sol−gel derived coating to a greater degree and, thus, access a higher fraction of the enzyme prior to introduction of the substrate. Hence, the

inverted lateral flow system, with incubation, was used for all subsequent applications of this sensing platform.

Figure 4A-a,A-c shows the dose-dependent inhibition responses of bendiocarb and carbaryl, respectively, while Figure 4A-b,A-d shows the semi log plots of the data in panels A-a and A-c, respectively. The insets (left panels) in Figure 4 show the images of the paper strips at each inhibitor concentration and clearly show a decrease in blue color intensity with increasing inhibitor concentration. Our data suggest that increasing concentrations of both bendiocarb and carbaryl progressively inhibit the activity of AChE. The apparent saturated inhibition concentration for both bendiocarb and carbaryl was found to be around 1 μM. On the basis of these results, the calculated IC_{50} values for bendiocarb and carbaryl to inhibit the activity of AChE by 50%, calculated by fitting the data to the Hill equation (SigmaPlot 2000), were 10 nM and 50 nM, respectively. In addition, the detection limits (concentration corresponding to the signal that was 3 standard deviations above the error on the mean signal from the blank) of bendiocarb and carbaryl were found to be ca. 1 and 10 nM, respectively. The results demonstrate that bendiocarb is a more potent pesticide for blocking AChE active sites than carbaryl. Our observations are in agreement with the results of previous studies of carbamate inhibition of AChE.[35] The limits of detection for the carbamates are well below the maximum allowable limit (MRL), as reported in the European Union pesticides database (0.02−0.05 mg/kg for meat or fruit).

Figure 4B-a,B-c shows the dose-dependent inhibition effects of paraoxon and malathion, respectively. Figure 4B-b,B-d represents the semi log plots of color intensity, corresponding to the same experiments in panels B-a and B-c, respectively. The IC_{50} values for paraoxon and malathion were approximately 50 nM while the LOD values were and 1 nM and 10 nM, respectively. The data are consistent with the results previously reported for organophosphate inhibition of AChE.[35] Also, the limits of detection of these organophosphate pesticides as obtained via our lateral flow paper-based assay system were well below the maximum allowable residual concentration (MRL), as reported by the European Union pesticides database (0.02−0.05 mg/kg meat or fruit), and the LOD for paraoxon (1 nM) was significantly better than that reported for our previous bioactive paper sensor that utilized the Ellman reaction (LOD = 100 nM), likely due to the ability to preincubate the inhibitor with the enzyme prior to introduction of the substrate. Overall, the data clearly show that the detection of the pesticides is possible with the naked eye, thereby avoiding the need for expensive and sophisticated instruments or electric power. Such a platform also makes it possible to perform remote sensing as qualitative estimations can be made on-site or images can be sent via camera phone to a central laboratory for quantitative assessment though image analysis.[11]

Assessing Sample Matrix Effects on Assay Performance. Milk and apple juice were spiked with varying levels of paraoxon to assess the effect of such sample matrices on assay performance and detection limits. Figure 5 shows a comparison between inhibition plots for standard solutions of paraoxon and for milk and apple juice samples that were spiked with the toxin. Initial attempts to assay apple juice directly were unsuccessful owing to the low pH of the sample matrix (pH = 3.6), which led to inactivation of the enzyme (see the supplementary Figure 1c in the Supporting Information). However, adjustment of the pH of apple juice to the range of 7 to 8 led to facile detection of the spiked pesticide. No pretreatment of the milk sample was required, as the pH of the matrix was close to 8.0. As shown in Figure 5, both the milk and apple juice matrices had a negligible effect on the limit of detection or the general shape of the response vs concentration, and the detection limits for paraoxon were estimated to be 1 nM for all samples.

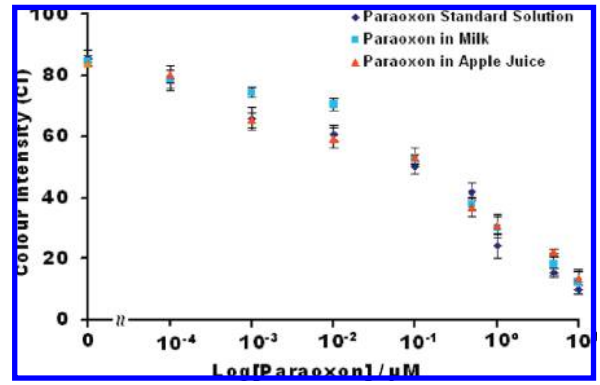

Figure 5. Matrix effects in the analysis of paraoxon in milk and apple juice samples. Color intensity decreased with the increased standard paraoxon concentration in milk and apple juice. All points are means ± s.d. of four independent measurements for each concentration. Apple juice samples were adjusted to a pH ~8 prior to analysis by addition of NaOH.

Paraoxon Analysis in Food Samples. To further evaluate the bioactive paper sensor, food samples including apples and head lettuce were sprayed with concentrated solutions of paraoxon (0−50 mM), and after drying, the samples were swabbed and the residue was tested. These concentrations (>1 mM) are similar to those typically used in spraying agricultural crops.[36,37] The results of the bioactive paper-based assays are shown in Figure 6a, where ~50% inhibition was observed when 10 μM paraoxon was sprayed, while almost complete inhibition was observed when 10 mM paraoxon was sprayed. Importantly, the data were highly reproducible even between different types of samples (apples vs lettuce), showing the utility of the assay for monitoring of pesticides on food.

To determine the actual concentration of paraoxon in the residues that were tested and assess the correlation to the initial calibration data provided above, bioactive paper assays were compared to an electrospray ionization-tandem mass spectrometry assay. For the ESI-MS/MS method, a calibration plot of paraoxon was produced by plotting peak area vs paraoxon concentration, which provided a linear response with a correlation coefficient of 0.996 (supplementary Figure 3 in the Supporting Information). This calibration plot was used to determine the concentration of paraoxon in swabs from sprayed apples, and the data was compared to the concentration determined with bioactive paper

(35) No, H.-Y.; Kim, Y. A.; Lee, Y. T.; Lee, H.-S. *Anal. Chem. Acta* **2007**, *594*, 37–43.
(36) Staiff, D. C.; Comer, S. W. *Bull. Environ. Contam. Toxicol.* **1975**, *14*, 135–139.
(37) Muttray, A.; Backer, G.; Jung, D.; Hill, G.; Letzel, S. *Toxicol. Lett.* **2006**, *162*, 219–224.
(38) Spencer, W. F.; Cllath, M. M.; Davis, K. R. *Bull. Environ. Contam. Toxicol.* **1975**, *14*, 265–272.

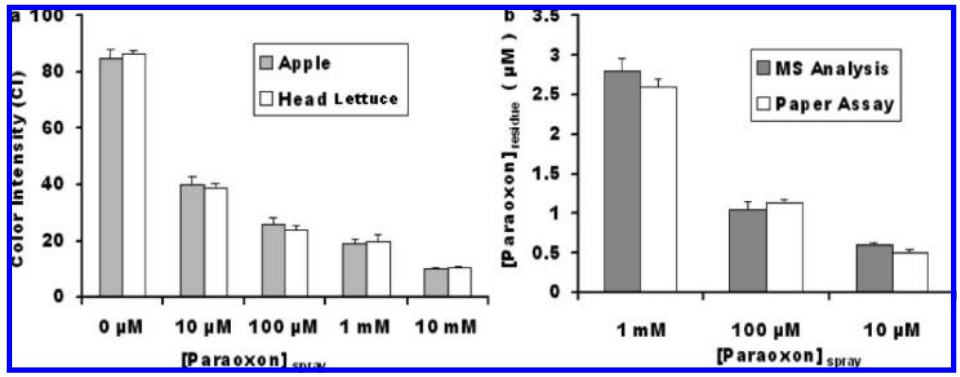

Figure 6. Detection of paraoxon on the surface of food samples, where different concentrations of paraoxon solution were sprayed on apple and head lettuce, respectively. (a) After air drying, the deposited paraoxon samples were collected and tested using the bioactive paper sensor. (b) Paraoxon residues (collected from apple samples) were assayed via the bioactive paper sensor strips and by a conventional ESI-MS/MS method. A comparison of the paper assay data with those of ESI-MS/MS analysis is shown. Data are means ± s.d. of three determinations.

strips using the calibration plot shown in Figure 4B-b. Figure 6b shows the comparison of paraoxon residue levels monitored both by the ESI-MS/MS method and the bioactive paper sensor strips. These two detection methods showed comparable results that were essentially within error, providing critical validation for the bioactive paper assay. Interestingly, the results showed that the level of paraoxon in the residue obtained from the swab did not correlate linearly with the amount in the initial spray solution, although a general trend of decreased paraoxon in the residue with decrease concentration in the initial spray was observed. The results obtained by the use of our reagentless paper sensor suggest that the optimized bioactive paper platform is very effective and sensitive and can play a very important role in both quantitative and qualitative measurement of pesticides.

A point that must be addressed for the AChE-based bioactive paper sensor is the potential for interferences that could arise from other AChE inhibitors. While it is unlikely that samples such as apple juice, milk, or lettuce would contain endogenous AChE inhibitors (indeed, our results presented above show that these samples did not contain endogenous inhibitors of AChE), it is possible that clinical samples might contain AChE inhibitors, which are often used to treat conditions such as Alzheimer's disease. As shown in supplementary Figure 4 (in the Supporting Information), the known AChE inhibitor galanthamine does produce a change in signal, as expected. This demonstrates that the sensor is able to detect any AChE inhibitor, not just pesticides, and cannot identify the specific inhibitor that is detected. However, the mass spectrometric procedure outlined above could be used as a secondary assay to identify an inhibitor that is detected in primary screening assays using the bioactive paper sensor.

Diminution of Paraoxon Residue Levels with Time. It is well-known that pesticides are readily absorbed through the skin and can be present on raw agricultural products and even table-ready foods. Even though such pesticides naturally degrade via hydrolysis mediated by physical, chemical, and biological processes, they persist long enough to be cause for concern. In order to investigate the degradation rate of paraoxon using our sensor strips, a standard paraoxon solution (1 mM) was sprayed on apples and the samples of paraoxon residue were collected each day, for one week. The results (supplementary Figure 5 in the Supporting Information) indicated that the paraoxon remained stable for at least 7 days with negligible degradation, which is in good agreement with previous literature reports.[34,38] Therefore, it is not safe to intake either vegetables or fruits directly from fields, where pesticides have been sprayed. Thus, the bioactive paper sensor could be a pivotal tool for assessment of low concentrations of class specific OP or CM pesticides, affecting both humans and animals.

Storage Stability of the Sensor. Our results (supplementary Figure 6 in the Supporting Information) demonstrated that the sensor strips retained >90% of their initial change in signal over a period of at least 1 month when stored at 4 °C, indicating that both the enzyme and the IPA reagent remained viable during storage. The observed stability of the enzyme when entrapped in silica is in agreement with previous reports[23,29] and shows that the reagentless bioactive paper sensor should have a sufficient shelf life to allow storage and shipping.

CONCLUSIONS

In this study, a reagentless lateral flow paper sensor for pesticides was developed by coating AChE and a suitable chromogenic substrate onto paper using either over spotting or inkjet printing of various "bioink" layers for detection of pesticides. The color intensity estimated by the naked eye or a digital camera is inversely proportional to the concentration of pesticides. Use of PVAm as a cationic capture agent on the paper significantly enhances the signal intensity, owing to its ability to trap and concentrate the anionic IDO^- product over a finite region, and also preserves the color response after several days of storage. The assay system showed a negligible matrix effect with pesticide-spiked milk and apple juice samples, provided that pH was adjusted to a suitable range close to pH 8.0. The sensor was also effective in analyzing pesticide residues collected from food samples without the need for electrical power or sophisticated instrumentation. Our experimental data show that both AChE and IPA entrapped between two biocompatible silica layers on paper retain full activity for at least 1 month when stored at 4 °C. The results are consistent with those of a conventional ESI-MS/MS method. On the basis of this study, we conclude that the bioactive paper-based assay platform is suitable for rapid screening of trace amount of OP and CM pesticides in the environment and food stuffs. Further efforts will focus on development of alternative enzyme-based sensors and multiplexed bioactive paper sensors. Our efforts in these areas will be reported in due course.

ACKNOWLEDGMENT

The authors thank the Natural Sciences and Engineering Research Council of Canada for funding this work through a network grant: *SENTINEL* Canadian Network for the Development and Use of Bioactive Paper. The authors also thank the Canada Foundation for Innovation and the Ontario Innovation Trust for support of this work. J.D.B. holds the Canada Research Chair in Bioanalytical Chemistry.

SUPPORTING INFORMATION AVAILABLE

Additional information as noted in text. This material is available free of charge via the Internet at http://pubs.acs.org.

Received for review July 30, 2009. Accepted September 14, 2009.

AC901714H